



SMALL OSCILLATIONS OF FINITELY DEFORMED ELASTIC NETWORKS

M.-P. WANG AND D. J. STEIGMANN*

Department of Mechanical Engineering, University of Alberta, Edmonton, Alberta, Canada
T6G 2G8

(Received 29 May 1996, and in final form 12 September 1996)

Linearized equations describing small motions superimposed on finitely deformed equilibrium configurations of elastic networks are derived. The theory is based on the so-called membrane model in which the fibres of the network are assumed to be continuously distributed to form a surface. A consistent linearization method is used to obtain equations of motion valid for arbitrary underlying equilibrium deformations. Modal analysis is performed for a sector of a one-parameter family of hyperbolic paraboloids with non-linearly elastic fibres, and the effect of geometric and material non-linearity on the frequency response of the network is quantified.

© 1997 Academic Press Limited

1. INTRODUCTION

The membrane theory of structural networks has been used for some time in the context of static analysis [1]. This theory is based on the conception that fibres of the network are continuously distributed, thereby forming an elastic surface. The model thus emerges as a special case of membrane theory. In simpler applications of linear versions of the theory, the equations of equilibrium may be solved by classical methods of applied mathematics such as Fourier analysis. Such a model thus yields a large amount of information for relative modest effort *vis-à-vis* a discrete network model having a large number of nodes. In numerical analysis, the use of the membrane model may appear to be a retrograde step, as the discrete-network equations are already in algebraic form for many cases of interest. However, a coarse discretization of the membrane equations often furnishes as much quantitative information as a direct analysis of an actual network containing many fibres. An equilibrium membrane theory valid for large deformations and strains of elastic networks was recently developed by Green and Shi [2] for two-dimensional deformations, and by Steigmann and Pipkin [3] for three-dimensional deformations of arbitrarily curved surfaces. A general numerical procedure for solving the non-linear equilibrium problem is discussed in reference [4].

In the context of dynamic analysis, the membrane theory of pre-stressed networks remains largely undeveloped, apart from certain special treatments intended for specific applications [5–8]. Moreover, existing works are based on models in which transverse motions are decoupled from the remaining components. The analysis is then typically concerned with transverse motion alone [5]. The validity of the de-coupled system is contingent upon the smallness of the deviation of the pre-stressed configuration from the

* Present address: Department of Mechanical Engineering, University of California at Berkeley, Berkeley, CA 94720, U.S.A.

plane. This limitation in turn restricts the applicability of the model. We do not impose any such restrictions in the present work.

In section 2 we recount the relevant aspects of the non-linear equilibrium theory of reference [3]. In particular, we demonstrate that the hyperbolic paraboloid furnishes an exact solution to the equilibrium equations, in the absence of distributed load, if the network is uniform in the sense that the fibre response functions do not depend explicitly on position. The linearization of the equations that describe superimposed motions is carried out in section 3, and the eigenproblem associated with oscillatory motions is derived. This is specialized to the case of small oscillations superimposed on a stressed hyperbolic paraboloid. The resulting system is not amenable to analytical solution, as the differential operator possesses variable coefficients the precise forms of which depend on the underlying equilibrium deformation and the functions that describe the constitutive response of the fibres.

In this work we use a finite difference method with co-ordinate mapping to reduce the eigenproblem to a standard algebraic form, which is then solved by the power method with deflation [9]. The procedure is described in section 4. The frequency response of a particular one-parameter family of hyperbolic paraboloids is studied in section 5.

2. FINITELY DEFORMED EQUILIBRIUM CONFIGURATIONS

In this section we present a concise development of the equilibrium equations for finite deformations of initially flat networks composed of two families of uniform elastic fibres. A general equilibrium theory for networks of arbitrary initial geometry is discussed in reference [3]. Thus consider a network that occupies a bounded region Ω of the (x_1, x_2) -plane with a piecewise smooth boundary $\partial\Omega$. Material points are identified with their position vectors $\mathbf{x} = x_\alpha \mathbf{e}_\alpha \in \Omega$, where Greek indices take values in $\{1, 2\}$ and $\{\mathbf{e}_1, \mathbf{e}_2\}$ is a fixed orthonormal basis. In a three-dimensional deformation of the network, the particle \mathbf{x} is displaced to the position $\mathbf{r}(\mathbf{x}) = r_i(\mathbf{x})\mathbf{e}_i$, where Latin indices range over $\{1, 2, 3\}$ and $\mathbf{e}_3 = \mathbf{e}_1 \times \mathbf{e}_2$. The gradient $\mathbf{F}(\mathbf{x})$ of the deformation $\mathbf{x} \rightarrow \mathbf{r}(\mathbf{x})$ is

$$\mathbf{F}(\mathbf{x}) = F_{ix} \mathbf{e}_i \otimes \mathbf{e}_x, \quad F_{ix} = r_{i,x}, \quad (1)$$

where the comma indicates a partial derivative with respect to x_α , summation on repeated indices is implied, and the notation $\mathbf{a} \otimes \mathbf{b}$ is used to denote the tensor product of vectors \mathbf{a} and \mathbf{b} .

The fibre trajectories on the reference plane are described by a pair of embedded unit tangent vector fields $\mathbf{L}(\mathbf{x}) = L_\alpha(\mathbf{x})\mathbf{e}_\alpha$ and $\mathbf{M}(\mathbf{x}) = M_\alpha(\mathbf{x})\mathbf{e}_\alpha$. We take the fibres to be orthogonal initially, so that $\mathbf{L} \cdot \mathbf{M} = 0$ and $\mathbf{L} \times \mathbf{M} = \mathbf{e}_3$ for all $\mathbf{x} \in \Omega$. Let $\lambda(\mathbf{x})$ and $\mu(\mathbf{x})$ be the stretches of the \mathbf{L} - and \mathbf{M} -fibres induced by the deformation. Then

$$\lambda(\mathbf{x}) = |\mathbf{FL}| \quad \text{and} \quad \mu(\mathbf{x}) = |\mathbf{FM}|. \quad (2)$$

The unit tangents, $\mathbf{l}(\mathbf{x})$ and $\mathbf{m}(\mathbf{x})$, to the images of the \mathbf{L} - and \mathbf{M} -fibres on the deformed surface, are given by

$$\lambda \mathbf{l} = \mathbf{FL} \quad \text{and} \quad \mu \mathbf{m} = \mathbf{FM}, \quad (3)$$

respectively. Since $\{\mathbf{L}, \mathbf{M}\}$ is an orthonormal basis at each $\mathbf{x} \in \Omega$, we may write

$$\delta_{\alpha\beta} = L_\alpha L_\beta + M_\alpha M_\beta, \quad (4)$$

where $\delta_{\alpha\beta}$ is the two-dimensional Kronecker delta. Then equations (4), (5) and the identity $F_{ix} = F_{i\beta}\delta_{\beta x}$ furnish the representation

$$\mathbf{F} = \mathbf{F}\mathbf{L}\otimes\mathbf{L} + \mathbf{F}\mathbf{M}\otimes\mathbf{M} = \lambda\mathbf{l}\otimes\mathbf{L} + \mu\mathbf{m}\otimes\mathbf{M}. \quad (5)$$

Next, let \mathbf{t} be the force in the network, measured per unit length of arc of a material curve on the reference plane. According to the theory developed in reference [3], this has the representation

$$\mathbf{t} = \mathbf{T}\nu, \quad (6)$$

where

$$\mathbf{T} = T_{ix}\mathbf{e}_i\otimes\mathbf{e}_x \quad (7)$$

is the unsymmetric Piola stress, and $\nu = \nu_x\mathbf{e}_x$ is the unit normal to the curve, lying to the right as the curve is traversed in the direction of increasing arc length. We remark that \mathbf{T} has dimensions of force/length in the present theory.

If an arbitrary part $D \subset \Omega$ of the network is in equilibrium with no distributed surface forces, then the integral of \mathbf{t} around its perimeter vanishes:

$$\oint_{\partial D} \mathbf{T}\nu \, ds = \mathbf{0}. \quad (8)$$

This condition, Green's theorem, and the arbitrariness of the region D lead to the pointwise equilibrium equation

$$\operatorname{div} \mathbf{T} = \mathbf{0}, \quad T_{ix,x} = 0, \quad \forall \mathbf{x} \in \Omega. \quad (9)$$

For wide-mesh networks, the Piola stress is given by the constitutive relation [3]

$$\mathbf{T} = f(\lambda)\mathbf{l}\otimes\mathbf{L} + g(\mu)\mathbf{m}\otimes\mathbf{M}, \quad T_{ix} = f(\lambda)l_iL_x + g(\mu)m_iM_x, \quad (10)$$

where f and g are the fibre forces, each measured per unit reference length of the orthogonal fibre family. The forces in the actual fibres are f/n and g/m , where n and m are the number of fibres per unit length crossing the \mathbf{M} - and \mathbf{L} -trajectories, respectively. It follows from equations (6) and (10) that \mathbf{t} lies in the tangent plane of the deformed surface at the particle \mathbf{x} . Thus the network does not support transverse shear forces.

In general, the Piola stress is work-conjugate to the deformation gradient in the sense that [3]

$$dW = \mathbf{T} \cdot d\mathbf{F}, \quad (11)$$

where W is the strain energy of the deformed surface per unit area of Ω , and dW is the increment in W associated with an increment $d\mathbf{F}$ of the deformation. Here the notation $\mathbf{A} \cdot \mathbf{B}$ is used to denote the scalar product, $A_{ix}B_{ix}$, of arbitrary tensors \mathbf{A} and \mathbf{B} . The form of the strain energy function may be deduced from equations (5) and (10) and the identities $\mathbf{l} \cdot d\mathbf{l} = 0$ and $\mathbf{m} \cdot d\mathbf{m} = 0$; the latter follow from the fact that \mathbf{l} and \mathbf{m} are unit vectors. Then the right side of equation (11) is $dW = f(\lambda) d\lambda + g(\mu) d\mu$, and we obtain

$$W = F(\lambda) + G(\mu), \quad (12)$$

where

$$F(\lambda) = \int f(\lambda) d\lambda, \quad G(\mu) = \int g(\mu) d\mu. \quad (13)$$

This implies that the response of a family of fibres is affected only by stretching of that family and that no energy or stress are required to shear the fibres. These conditions were imposed *a priori* in reference [3] to derive the present model from the general theory of elastic membranes.

In the remainder of this work we take the fibres to be oriented along the (x_1, x_2) -axes on the reference plane, so that

$$L_x = \delta_{x_1} \quad \text{and} \quad M_x = \delta_{x_2}. \quad (14)$$

On combining these with equations (9) and (10), we derive the equilibrium equation

$$[f(\lambda)l_i]_{,x} \delta_{x_1} + [g(\mu)m_i]_{,a} \delta_{x_2} = 0, \quad (15)$$

which is equivalent to

$$[\lambda^{-1}f(\lambda)\mathbf{r}_{,1}]_1 + [\mu^{-1}g(\mu)\mathbf{r}_{,2}]_2 = \mathbf{0}. \quad (16)$$

Here we have used equations (1)–(3) and (14) to deduce that

$$\lambda \mathbf{l} = \mathbf{F}\mathbf{e}_1 = \mathbf{r}_{,1}, \quad \mu \mathbf{m} = \mathbf{F}\mathbf{e}_2 = \mathbf{r}_{,2}; \quad \lambda = |\mathbf{r}_{,1}|, \quad \mu = |\mathbf{r}_{,2}|. \quad (17)$$

The general hyperbolic paraboloid, defined by

$$r_1 r_2 / r_3 = \text{constant}, \quad (18)$$

furnishes a solution to equations (16) and (17) for all elastically uniform networks; i.e., for all fibre response functions $f(\lambda)$ and $g(\mu)$ that do not depend on \mathbf{x} explicitly [3]. To see this, we write equation (18) in the parametric form

$$\mathbf{r}(\mathbf{x}) = ax_1 x_2 \mathbf{e}_3 + bx_1 \mathbf{e}_1 + cx_2 \mathbf{e}_2, \quad (19)$$

where a, b and c are constants with $a \neq 0$. Then equation (18) is satisfied with the constant equal to bc/a . Moreover, $\mathbf{r}_{,1}$ and λ are independent of x_1 , and $\mathbf{r}_{,2}$ and μ are independent of x_2 , so equation (16) is automatically satisfied. The fibre stretches associated with equation (19) are

$$\lambda(x_2) = (a^2 x_2^2 + b^2)^{1/2} \quad \text{and} \quad \mu(x_1) = (a^2 x_1^2 + c^2)^{1/2}. \quad (20)$$

3. SMALL SUPERIMPOSED MOTIONS

We derive the equations that describe a small amplitude motion superimposed on a finite equilibrium deformation $\mathbf{r}(\mathbf{x})$. Thus let $\mathbf{r}^*(\mathbf{x}, t)$ be a finite motion of the network, and let

$$\mathbf{r}^*(\mathbf{x}, t) = \mathbf{r}(\mathbf{x}) + \varepsilon \mathbf{u}(\mathbf{x}, t), \quad (21)$$

where $\mathbf{u}(\mathbf{x}, t)$ and its derivatives are of order $O(1)$ in magnitude after suitable non-dimensionalization, and ε is a small parameter. This parameter is used here as a device for distinguishing linear terms from non-linear terms in the limit of infinitesimally small motions. After linearization of the pertinent equations has been accomplished, ε may be set equal to unity without loss of generality, with the understanding that the resulting model applies when $\mathbf{u}(\mathbf{x}, t)$ and its derivatives with respect to \mathbf{x} and t are very small in magnitude compared to unity.

Let $\rho(\mathbf{x})$ be the mass of the network per unit area of the reference plane Ω . The equation of motion of an arbitrary part $D \subset \Omega$ is

$$\oint_{\partial D} \mathbf{T}^* \cdot \mathbf{v} \, ds = \frac{\partial}{\partial t} \int_D \rho \frac{\partial}{\partial t} \mathbf{r}^* \, dA, \quad (22)$$

where \mathbf{T}^* is the stress associated with the motion \mathbf{r}^* . The argument that led to equation (9) now yields the local equations

$$\operatorname{div} \mathbf{T}^* = \rho \partial^2 \mathbf{r}^* / \partial t^2; \quad T_{ix,x}^* = \rho \partial^2 r_i^* / \partial t^2. \quad (23)$$

Formally, linear equations for the small superimposed motion may be obtained by expanding the stress about the equilibrium stress \mathbf{T} and retaining lowest order terms in the parameter ε . Thus,

$$T_{ix}^* = T_{ix} + \varepsilon \dot{T}_{ix} + o(\varepsilon), \quad (24)$$

where the superimposed dot is used to denote a derivative with respect to ε , evaluated at $\varepsilon = 0$. Substitution of equations (24) and (21) into equation (23) yields

$$T_{ix,x} + \varepsilon \dot{T}_{ix,x} + o(\varepsilon) = \varepsilon \rho \partial^2 u_i / \partial t^2. \quad (25)$$

Dividing by ε , invoking equation (9) and letting $\varepsilon \rightarrow 0$, we obtain the linearization

$$\operatorname{div} \dot{\mathbf{T}} = \rho \partial^2 \mathbf{u} / \partial t^2, \quad \dot{T}_{ix,x} = \rho \partial^2 u_i / \partial t^2. \quad (26)$$

It is convenient to introduce stress vectors $\dot{\mathbf{T}}_\alpha$ such that

$$\dot{\mathbf{T}} = \dot{\mathbf{T}}_\alpha \otimes \mathbf{e}_\alpha. \quad (27)$$

Then $\dot{\mathbf{T}}_\alpha = \dot{\mathbf{T}}\mathbf{e}_\alpha = \dot{T}_{ix}\mathbf{e}_i$, and equation (26) may be written

$$\dot{\mathbf{T}}_{\alpha,\alpha} = \rho \partial^2 \mathbf{u} / \partial t^2. \quad (28)$$

To obtain expressions for $\dot{\mathbf{T}}_\alpha$ in terms of the motion $\mathbf{u}(\mathbf{x}, t)$, we first use equation (3) to rewrite equation (10) in the form

$$T_{ix} = F_{i\beta} [\lambda^{-1} f(\lambda) L_\beta L_\alpha + \mu^{-1} g(\mu) M_\beta M_\alpha]. \quad (29)$$

Then

$$\dot{T}_{ix} = \dot{F}_{i\beta} (\lambda^{-1} f(\lambda) L_\beta L_\alpha + \mu^{-1} g(\mu) M_\beta M_\alpha) + F_{i\beta} [(\dot{\lambda}^{-1} f) L_\beta L_\alpha + (\mu^{-1} \dot{g}) M_\beta M_\alpha], \quad (30)$$

where $\dot{F}_{ix} = u_{i,x}$ is the gradient of the small superimposed displacement. We note that $\dot{\mathbf{L}}$ and $\dot{\mathbf{M}}$ vanish because \mathbf{L} and \mathbf{M} are material vectors.

To proceed it is necessary to express $\dot{\lambda}$ and $\dot{\mu}$ in terms of \dot{F}_{ix} . To this end we use equation (2) to obtain

$$\lambda^2 = F_{ix} F_{i\beta} L_\alpha L_\beta \quad \text{and} \quad \mu^2 = F_{ix} F_{i\beta} M_\alpha M_\beta. \quad (31)$$

Then

$$\dot{\lambda} = \frac{1}{2\lambda} (\dot{F}_{ix} F_{i\beta} + F_{ix} \dot{F}_{i\beta}) L_\alpha L_\beta = \frac{1}{\lambda} \dot{F}_{ix} F_{i\beta} L_\alpha L_\beta, \quad (32)$$

with a similar expression for $\dot{\mu}$. From equation (3) it then follows that

$$\dot{\lambda} = l_i L_\alpha u_{i,x} \quad \text{and} \quad \dot{\mu} = m_i M_\alpha u_{i,x}, \quad (33)$$

where \mathbf{l} and \mathbf{m} are the unit tangents to the deformed fibres on the equilibrium surface $\mathbf{r}(\mathbf{x})$. Substitution of equations (3) and (33) into equation (30) results in

$$\begin{aligned} \dot{T}_{ix} = & \{ [f'(\lambda) - \lambda^{-1} f(\lambda)] l_i l_j + \lambda^{-1} f(\lambda) \delta_{ij} \} L_\alpha L_\beta u_{j,\beta} \\ & + \{ [g'(\mu) - \mu^{-1} g(\mu)] m_i m_j + \mu^{-1} g(\mu) \delta_{ij} \} M_\alpha M_\beta u_{j,\beta}, \end{aligned} \quad (34)$$

where δ_{ij} is the three-dimensional Kronecker delta. Then the stress vectors are

$$\dot{\mathbf{T}}_\alpha = \mathbf{E}_{\alpha\beta} \mathbf{u}_{,\beta}, \quad (35)$$

where

$$\begin{aligned} \mathbf{E}_{\alpha\beta} = & \{ [f'(\lambda) - \lambda^{-1}f(\lambda)] \mathbf{I} \otimes \mathbf{I} + \lambda^{-1}f(\lambda) \mathbf{I}_j \} L_\alpha L_\beta \\ & + \{ [g'(\mu) - \mu^{-1}g(\mu)] \mathbf{m} \otimes \mathbf{m} + \mu^{-1}g(\mu) \mathbf{I}_j \} M_\alpha M_\beta, \end{aligned} \quad (36)$$

and

$$\mathbf{I} = \delta_{ij} \mathbf{e}_i \otimes \mathbf{e}_j \quad (37)$$

is the unit tensor for three-space. The general linear equation of motion for superimposed displacements is thus given by

$$(\mathbf{E}_{\alpha\beta} \mathbf{u}_{,\beta})_{,\alpha} = \rho \partial^2 \mathbf{u} / \partial t^2. \quad (38)$$

In the remainder of this work we consider networks having uniform mass density ($\rho = \text{constant}$) in the reference configuration Ω .

To study the frequency response of the network, we consider motions of the form

$$\mathbf{u}(\mathbf{x}, t) = \mathbf{v}(\mathbf{x}) \exp(i\omega t). \quad (39)$$

Then equation (38) yields the eigenproblem

$$(\mathbf{E}_{\alpha\beta} \mathbf{v}_{,\beta})_{,\alpha} + \rho\omega^2 \mathbf{v} = \mathbf{0}. \quad (40)$$

The coefficients in this equation are determined by the underlying equilibrium deformation $\mathbf{r}(\mathbf{x})$. For the deformation described by equation (19), it follows from equations (14), (17), (20) and (36) that

$$\mathbf{E}_{12} = \mathbf{E}_{21} = \mathbf{0} \quad \text{and} \quad \mathbf{E}_{11,1} = \mathbf{E}_{22,2} = \mathbf{0}. \quad (41)$$

Equation (40) thus reduces to

$$\mathbf{E}_{11}(x_2) \mathbf{v}_{,11} + \mathbf{E}_{22}(x_1) \mathbf{v}_{,22} + \rho\omega^2 \mathbf{v} = \mathbf{0}. \quad (42)$$

An equivalent system of three coupled scalar equations may be derived by projection on to the elements of the fixed orthonormal basis $\{\mathbf{e}_i\}$. We do not exhibit this system explicitly here, however.

An *a priori* restriction on the eigenvalues may be derived by scalar-multiplying equation (40) with \mathbf{v} :

$$(\mathbf{v} \cdot \mathbf{E}_{\alpha\beta} \mathbf{v}_{,\beta})_{,\alpha} + \rho\omega^2 |\mathbf{v}|^2 = 0. \quad (43)$$

The first term may be written in the form

$$(\mathbf{v} \cdot \mathbf{E}_{\alpha\beta} \mathbf{v}_{,\beta})_{,\alpha} - (\mathbf{E}_{\alpha\beta} \mathbf{v}_{,\beta}) \cdot \mathbf{v}_{,\alpha}. \quad (44)$$

Integration over the reference plane Ω and application of Green's theorem then yields

$$\rho\omega^2 \int_{\Omega} |\mathbf{v}(\mathbf{x})|^2 dA = \int_{\Omega} (\mathbf{E}_{\alpha\beta} \mathbf{v}_{,\beta}) \cdot \mathbf{v}_{,\alpha} dA - \int_{\partial\Omega} \mathbf{v} \cdot (\mathbf{E}_{\alpha\beta} \mathbf{v}_{,\beta}) v_\alpha ds, \quad (45)$$

where v_α are the components of the exterior unit normal to the curve $\partial\Omega$.

For pure displacement problems with time-independent data, the boundary values of the deformation are fixed and the superimposed motion is required to vanish on the boundary. It follows that $\mathbf{v}(\mathbf{x}) = \mathbf{0}$ on $\partial\Omega$; the boundary integral in equation (45) thus vanishes identically. Furthermore, with the aid of equation (36) it is possible to show that $(\mathbf{E}_{\alpha\beta} \mathbf{v}_{,\beta}) \cdot \mathbf{v}_{,\alpha} > 0$ for all non-zero $\mathbf{v}_{,\alpha}$ if and only if [10]

$$f(\lambda) > 0, \quad g(\mu) > 0, \quad f'(\lambda) > 0, \quad g'(\mu) > 0. \quad (46)$$

For typical fibre response functions, including those considered in section 5 below, these inequalities are automatically satisfied whenever $\lambda > 1$ and $\mu > 1$. Therefore, sufficient conditions for the positive definiteness of the right side of equation (45) are: $\lambda(\mathbf{x}) > 1$, $\mu(\mathbf{x}) > 1$, for all $\mathbf{x} \in \Omega$. These imply that ω^2 is strictly positive, which in turn implies that the configuration $\mathbf{r}(\mathbf{x})$ is linearly stable in the sense that the superimposed motion is a bounded oscillation. In particular, the stability of the hyperbolic paraboloid under fixed displacement conditions on $\partial\Omega$ may be guaranteed by requiring that $b > 1$ and $c > 1$ in equations (19) and (20), provided that these restrictions are compatible with the data.

Dimensionless equations are obtained by introducing a length scale L and a modulus E , the latter having dimensions of force/length. These are used to define the dimensionless variables and functions

$$\hat{x}_\alpha = x_\alpha/L, \quad \hat{\mathbf{v}} = \mathbf{v}/L, \quad \hat{\mathbf{r}} = \mathbf{r}/L, \quad \hat{a} = aL$$

and

$$\hat{f}(\lambda) = f(\lambda)/E, \quad \hat{g}(\mu) = g(\mu)/E, \quad \hat{\mathbf{E}}_{\alpha\beta} = \mathbf{E}_{\alpha\beta}/E,$$

where a is the parameter in equation (19). We note that the parameters b and c in the latter equation are already dimensionless. Substituting into equation (42) and dividing by E/L , we obtain a dimensionless system that is identical in form to equation (42), with the exception that $\rho\omega^2$ is replaced by $\hat{\omega}^2$, where

$$\hat{\omega} = (\rho/E)^{1/2}L\omega. \tag{47}$$

We remark that the coefficients in equation (42) involve \mathbf{x} in a manner that depends on the non-homogeneous deformation (19) and the particular fibre-response functions considered. Thus the eigenproblem is generally not amenable to analytical solution.

4. NUMERICAL SOLUTION

We solve the eigenproblem by applying spatial finite-differencing to equation (42), and then using a conventional power method to find the frequencies and mode vectors of the resulting algebraic system.

In typical applications, the boundaries of the domain Ω may be irregular and may not coincide with co-ordinate curves. This difficulty is addressed by using a co-ordinate transformation to map the region Ω to the interior of a square region in a parameter plane Ω' , which then serves as the domain of the discretized problem.

The particular method used here is the orthogonal mapping algorithm of Ryskin and Leal [11], which is based on the identities

$$\Delta x_\alpha = 0, \quad \alpha = 1, 2, \tag{48}$$

where $\Delta(\cdot)$ is the two-dimensional Laplacian. We introduce orthogonal curvilinear co-ordinates ξ_1 and ξ_2 to cover the region Ω . These are rectangular co-ordinates in Ω' , chosen such that $\Omega' = [0, 1] \times [0, 1]$, and we use them to write equation (48) in the form [11]

$$F \frac{\partial^2 x_\alpha}{\partial \xi_1^2} + \frac{1}{F} \frac{\partial^2 x_\alpha}{\partial \xi_2^2} + \frac{\partial F}{\partial \xi_1} \frac{\partial x_\alpha}{\partial \xi_1} - \frac{1}{F^2} \frac{\partial F}{\partial \xi_2} \frac{\partial x_\alpha}{\partial \xi_2} = 0, \quad \alpha = 1, 2, \tag{49}$$

where

$$F(\xi_1, \xi_2) = H_2/H_1, \quad H_1 = \left[\left(\frac{\partial x_1}{\partial \xi_1} \right)^2 + \left(\frac{\partial x_2}{\partial \xi_1} \right)^2 \right]^{1/2}, \quad H_2 = \left[\left(\frac{\partial x_1}{\partial \xi_2} \right)^2 + \left(\frac{\partial x_2}{\partial \xi_2} \right)^2 \right]^{1/2}. \tag{50}$$

Equations (49) and (50) yield a non-linear generating system for the functions $x_\alpha(\xi_1, \xi_2)$. This is augmented by Dirichlet conditions that specify the correspondences of points on $\partial\Omega'$ and $\partial\Omega$. The equations are discretized by using standard first and second order central differences, and the resulting non-linear algebraic system is solved iteratively on a uniform square grid. Here we follow the *weak constraint* method suggested in reference [11]. (a) Specify an initial guess for the discrete fields $x_\alpha(\xi_1, \xi_2)$. This is accomplished by the *four-point weighted average* scheme of Thompson *et al.* [12]. (b) Compute the initial guess for the function $F(\xi_1, \xi_2)$ at the nodes using the discrete form of equation (50). (c) Use successive over-relaxation iteration [12], together with the Dirichlet data, to obtain the next iterate of $x_\alpha(\xi_1, \xi_2)$ from the discrete versions of equation (49). (d) Compute the boundary values of $F(\xi_1, \xi_2)$ from equation (50), and solve the discrete form of Laplace's equation,

$$\frac{\partial^2 F}{\partial \xi_1^2} + \frac{\partial^2 F}{\partial \xi_2^2} = 0, \quad (51)$$

for the nodal values of F in Ω' . (e) Return to step (c) and continue until convergence is achieved.

Once the grid has been generated, it remains to transform the dimensionless form of equation (42) to a system with ξ_1 and ξ_2 as independent variables. This is accomplished by applying the derivative formulae

$$\frac{\partial G}{\partial x_1} = \left(\frac{\partial G}{\partial \xi_1} \frac{\partial x_2}{\partial \xi_2} - \frac{\partial G}{\partial \xi_2} \frac{\partial x_2}{\partial \xi_1} \right) / J, \quad \frac{\partial G}{\partial x_2} = \left(-\frac{\partial G}{\partial \xi_1} \frac{\partial x_1}{\partial \xi_2} + \frac{\partial G}{\partial \xi_2} \frac{\partial x_1}{\partial \xi_1} \right) / J \quad (52)$$

to equation (42), where G is an arbitrary function and

$$J = \frac{\partial x_1}{\partial \xi_1} \frac{\partial x_2}{\partial \xi_2} - \frac{\partial x_1}{\partial \xi_2} \frac{\partial x_2}{\partial \xi_1} \quad (53)$$

is the Jacobian determinant of the transformation from (ξ_1, ξ_2) to (x_1, x_2) . Formulae for the second derivatives with respect to x_1 and x_2 follow from repeated application of equations (52) and (53). These formulae are recorded explicitly in reference [12].

Derivatives with respect to ξ_1 and ξ_2 in the transformed version of equation (42) are then approximated by central difference operators to derive the algebraic problem

$$(A)\{v\} = A\{v\}, \quad (54)$$

where $A(>0)$ is the square of the dimensionless frequency defined in equation (47),

$$\{v\} = \{v_{1(1)}, v_{1(2)}, \dots, v_{1(n)}; v_{2(1)}, v_{2(2)}, \dots, v_{2(n)}; v_{3(1)}, v_{3(2)}, \dots, v_{3(n)}\}^T \quad (55)$$

is the mode vector, $v_{i(j)}$ is the i th component of $\mathbf{v} = v_i \mathbf{e}_i$ at the j th node, n is the number of interior nodes in the mesh, and (A) is the symmetric matrix representing the discrete form of the differential operator in equation (42).

The frequencies and associated mode vectors are obtained by solving equation (54) using the well known power method with deflation [9]. In the next section we exhibit the lowest frequencies and modes for a particular illustrative example. These were obtained by solving the system

$$(A)^{-1}\{v\} = A^{-1}\{v\}. \quad (56)$$

Application of the power and deflation methods to this system yields the squared frequencies in ascending order.

5. EXAMPLE

As an illustrative example, we consider a sector of a hyperbolic paraboloid with edges defined by

$$r_1 - r_2 = A, \quad r_1 - r_2 = -A, \quad r_3 = B, \quad (57)$$

where A and B are constants to be specified. According to equations (18) and (19), the third of equations (57) is equivalent to

$$r_1 r_2 = (bc/a)B, \quad (58)$$

where a , b and c are the parameters that define the equilibrium surface. We take the points of intersection of adjacent boundary curves to be located at the four points with co-ordinates

$$(r_1, r_2) = \frac{1}{2}(-A + C, A + C), \frac{1}{2}(-A - C, A - C), \frac{1}{2}(A + C, -A + C), \\ \frac{1}{2}(A - C, -A - C),$$

where

$$C = [A^2 + 4B(bc/a)]^{1/2}. \quad (59)$$

The images of the boundary curves on the reference plane are obtained by substituting $r_1 = bx_1$ and $r_2 = cx_2$ (see equation (19)):

$$bx_1 - cx_2 = A, \quad bx_1 - cx_2 = -A, \quad x_1 x_2 = B/a. \quad (60)$$

We choose the length scale for the non-dimensionalization scheme to be the perpendicular distance between the parallel lines described by equations (60a, b):

$$L = A(b^2 + c^2)^{1/2}/bc. \quad (61)$$

The length of these lines is

$$l = C(b^2 + c^2)^{1/2}/bc. \quad (62)$$

In terms of dimensionless co-ordinates, the curves (60) are given by

$$b\hat{x}_1 - c\hat{x}_2 = \hat{A}, \quad b\hat{x}_1 - c\hat{x}_2 = -\hat{A}, \quad \hat{x}_1 \hat{x}_2 = \hat{B}/\hat{a}, \quad (63)$$

where $\hat{A} = A/L = bc/(b^2 + c^2)^{1/2}$, $\hat{B} = B/L$ and \hat{a} is the parameter defined prior to equation (47). It follows from equations (59), (60) and (62) that

$$\hat{B}/\hat{a} = (\hat{l}^2 - 1)\hat{A}^2/4bc, \quad (64)$$

where $\hat{l} = l/L$. Thus the mapping from the hyperbolic paraboloid to the dimensionless (\hat{x}_1, \hat{x}_2) -plane is completely determined by the parameters b , c and \hat{l} . The region of this plane enclosed by the boundary curves is shown in Figure 1 for $b = c = 1.1$ and $\hat{l} = 1.5$. Also shown is a 25×25 mesh generated by the mapping algorithm of Ryskin and Leal. This region is taken to be the reference configuration for the network. We note that the fibres are aligned with the ordinate and abscissa. The corresponding sector of the deformed equilibrium surface is shown in Figure 2.

The computation of the frequency response of the pre-stressed network requires the specification of the fibre response functions. We take these to be

$$f(\lambda) = E\lambda(1 - \lambda^{-3}), \quad g(\mu) = E\mu(1 - \mu^{-3}), \quad (65)$$

where E is a positive constant. These functions are often used to approximate the tensile response of polymeric fibres at small to moderate strain. The constant E is identified with

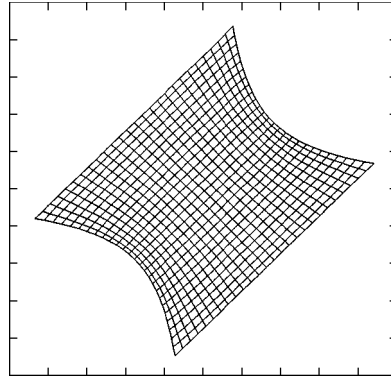


Figure 1. The stress-free reference configuration overlaid with a 25×25 mesh.

the modulus in the non-dimensionalization scheme of section 3. Of course, it is possible to consider fibre families having different moduli and different functional dependence on the stretches, but we do not do so here.

For the fixed-displacement problem ($\mathbf{v} = \mathbf{0}$ on $\partial\Omega$), the first three vibrational modes associated with $\hat{a} = 0.6$ are shown in Figures 3(a)–(c), respectively. The corresponding dimensionless frequencies are 2.071, 3.119 and 3.387.

A sequence of computations performed on successively finer grids indicates that convergence of the first three frequencies is achieved using a mesh somewhat coarser than the one indicated.

The variation of the fundamental frequency versus the dimensionless parameter \hat{a} associated with the equilibrium configuration is shown in Figure 4. We note that each value of the parameter corresponds to the same material network, as the domain of the network in the reference plane is fixed for particular values of the constants b , c and \hat{l} . Adjustment of \hat{a} thus requires adjustment of \hat{B} such that the right side of equation (64) remains fixed. This means that an increase of \hat{a} corresponds to a more pronounced three-dimensional deformation of the hyperbolic paraboloid. This also induces increased stretching of the fibres (see equation (20)) and an attendant increase in the fibre tensions. The combined effect of this geometric and material stiffening is reflected in the observed increase of the fundamental frequency.

Finally, as the present example has no analytical solution available for comparison, we have used the foregoing method to solve the classical vibrating membrane problem,

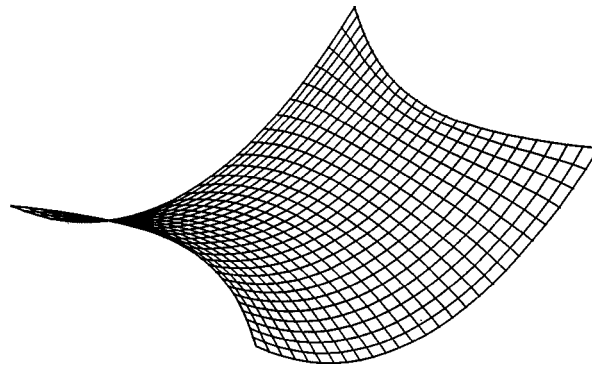


Figure 2. The equilibrium hyperbolic paraboloid corresponding to $\hat{a} = 0.6$.

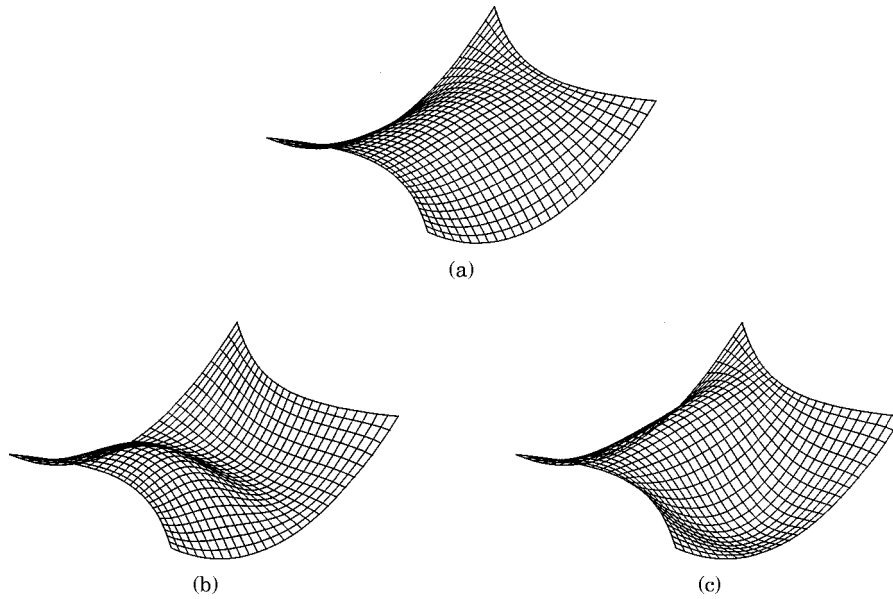


Figure 3. (a) The fundamental mode ($\hat{\omega}_1 = 2.071$). (b) The second mode ($\hat{\omega}_2 = 3.119$). (c) The third mode ($\hat{\omega}_3 = 3.387$).

without grid-mapping, on the unit square. This problem may be recovered from the present formulation by taking $a = 0$ and $b = c (> 1)$ in equation (19). It is straightforward to show that the \mathbf{e}_3 -component of equation (42) decouples from the remaining components in this case, and is identical in form to the classical problem. The first five frequencies were computed on 12×12 , 15×15 and 17×17 meshes. Monotone convergence to the analytical frequencies was observed in every instance, with faster convergence occurring in the lower modes. The relative error in the fifth frequency was 1% on the 17×17 grid.

To test the grid-mapping algorithm, we repeated the calculation on the unit circle. The first three modes were obtained using 12×12 and 15×15 meshes. Similar convergence behaviour was observed. The relative error in the third frequency was 1.32% with a 15×15 mesh. In contrast, the third frequency for the unit square was calculated with an

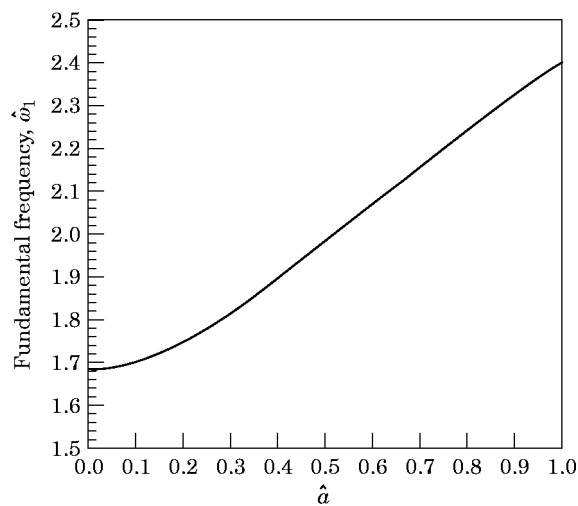


Figure 4. The fundamental frequency of a one-parameter family of hyperbolic paraboloids: $b = c = 1.1$.

error of 0.6% using the same mesh density. The difference is due to truncation errors associated with the mesh-generation algorithm. As expected, the effect of this additional source of error diminished with mesh refinement.

Finally, we remark that in the example considered, the extra computational effort associated with the grid-mapping algorithm is significant when compared with that required for the basic eigenanalysis, particularly if one is interested only in the lower modes. However, this statement is qualified by the fact that no effort was made in this preliminary work to optimize the computations. Alternative mesh-generation procedures should be explored before applying the foregoing method to the modal analysis of large scale network structures. This is beyond the scope of the present work, which is concerned mainly with the theoretical development and the presentation of illustrative examples.

6. SUMMARY

In this work we have obtained the consistent linearization of the equations of motion in the membrane theory of elastic networks. The resulting system is fully coupled with variable coefficients, the precise forms of which depend on the fibre response functions and the underlying equilibrium deformation.

The frequency response of a pre-stressed hyperbolic paraboloid was computed using finite differences together with a grid-mapping method for networks with irregular boundaries. Quantitative results were obtained for the natural frequencies, and the fundamental frequency of a one-parameter family of hyperbolic paraboloids was obtained over a range of values of the parameter, in respect of a certain class of fibre response functions.

ACKNOWLEDGMENTS

We gratefully acknowledge the support of the Natural Sciences and Engineering Research Council of Canada. M.W. acknowledges the partial support of a Province of Alberta scholarship for studies leading to the M.Sc. degree.

REFERENCES

1. F.-K. SCHLEYER 1967 in *F. Otto's Tensile Structures, Part 2, Vol. 2*. Cambridge, MA: MIT Press. Analysis of cables, cable nets and cable structures.
2. W. A. GREEN and J. SHI 1990 *Quarterly Journal of Mechanics and Applied Mathematics* **43**, 317–333. Plane deformations of membranes formed with elastic cords.
3. D. J. STEIGMANN and A. C. PIPKIN 1991 *Philosophical Transactions of the Royal Society of London* **A335**, 419–454. Equilibrium of elastic nets.
4. E. M. HASEGANU and D. J. STEIGMANN 1996 *Computational Mechanics* **17**, 359–373. Equilibrium analysis of finitely deformed elastic networks.
5. M. IRVINE 1981 *Cable Structures*. New York: Dover; 1992 edition.
6. S. SHORE and B. CHAUDHARI 1972 *Proc. Int'l. Assoc. Bridge and Structural Engng., 9th Congress*, 445–451. Amsterdam. Free vibrations of cable networks utilizing analogous membrane.
7. K. G. SANGSTER and B. DEV. BATCHELOR 1974 in *Computational Methods in Nonlinear Mechanics*. J. T. Oden., E. B. Becker., R. R. Craig., R. S. Dunham., C. P. Johnson and W. L. Oberkampf, (editors), 301–310. Austin, TX: TICOM. Nonlinear dynamic analysis of 3-D cable networks.
8. H. MOLLMANN 1972 *Proceedings of an IASS Pacific Symposium on Tension Structures and Space Frames, Tokyo and Kyoto*, 289–304. Analytical solution for a cable net over a rectangular plan.
9. L. MEIROVITCH 1980 *Computational Methods in Structural Dynamics*. Alphen aan der Rijn: Sijthoff & Noordhoff.

10. D. J. STEIGMANN 1992 *Institute for Mathematics and its Applications, Journal of Applied Mathematics* **48**, 195–215. Equilibrium of prestressed networks.
11. G. RYSKIN and L. G. LEAL 1983 *Journal of Computational Physics* **50**, 71–100. Orthogonal mapping.
12. J. F. THOMPSON, F. C. THAMES and C. W. MASTIN 1976 *NASA CR-27229*. Boundary-fitted curvilinear coordinate systems for solution of partial differential equations on fields containing any number of arbitrary two-dimensional bodies.